JETP Letters, Vol. 75, No. 7, 2002, pp. 336–341. From Pis'ma v Zhurnal Éksperimental'noĭ i Teoreticheskoĭ Fiziki, Vol. 75, No. 7, 2002, pp. 407–412.

Density of States in a Mesoscopic SNS Junction[1]

P. M. Ostrovsky*, M. A. Skvortsov, and M. V. Feigel'man

Landau Institute for Theoretical Physics, Russian Academy of Sciences, Moscow, 117940 Russia

**e-mail: ostrov@itp.ac.ru*

Received February 28, 2002

The semiclassical theory of proximity effects predicts a gap $E_g \sim \hbar D/L^2$ in the excitation spectrum of a long diffusive superconductor/normal-metal/superconductor (SNS) junction. Mesoscopic fluctuations lead to anomalously localized states in the normal part of the junction. As a result, a nonzero, yet exponentially small, density of states (DOS) appears at energies below E_g. In the framework of the supermatrix nonlinear σ model, these prelocalized states are due to the instanton configurations with broken supersymmetry. The exact result for the DOS near the semiclassical threshold is found, provided the dimensionless conductance of the normal part G_N is large. The case of poorly transparent interfaces between the normal and superconductive regions is also considered. In this limit, the total number of subgap states may be large. © *2002 MAIK "Nauka/Interperiodica".*

PACS numbers: 73.21.-b; 74.50.+r; 74.80.Fp

1. Introduction. It has recently been shown within several different although related contexts that the excitation energy spectrum of superconducting–normal (SN) chaotic hybrid structures [1, 2] and superconductors with magnetic impurities [3, 4] does not possess a *hard gap*, as predicted by a number of papers [5–8] using the semiclassical theory of superconductivity [9–11]. With mesoscopic fluctuations taken into account, the phenomenon of a *soft gap* appears: the density of states is nonzero at all energies, but it decreases exponentially rapidly below the semiclassical threshold $E_g \sim \hbar/\tau_c$, with τ_c being the characteristic dwell time in the N region. In particular, for diffusive systems perfectly connected to a superconductor, E_g has the order of the Thouless energy E_{Th} in the N region [5, 6].

The first result in this direction was obtained in [1], where the subgap density of states (DOS) in a quantum dot was studied by employing the universality hypothesis and predictions [12] of the random-matrix theory (RMT) [13]. Later on, the tail states in a superconductor with magnetic impurities were analyzed in [3, 4] on the basis of the supersymmetric nonlinear σ-model method [14] extended to include superconducting paring [15].

A fully microscopic approach to the problem of the subgap states in diffusive normal-metal/superconductor (NS) systems was developed in [2] in the framework of the supersymmetric σ model similar to that employed in [3, 4]. Physically, the low-lying excitations in SN structures are due to anomalously localized eigenstates [16] in the N region. From the mathematical side, nonzero DOS at $E < E_g$ comes about when nontrivial field configurations—instantons—are taken into account in the σ-model functional integral. As shown in [2], at $E \approx E_g$ there are two different types of instantons, their actions being different by a factor of 2. The main contribution to the exponentially small subgap DOS is determined by the Gaussian integral near the least-action instanton.

For a planar (quasi-1D) superconductor/normal-metal/superconductor (SNS) junction with ideally transparent SN interfaces, the DOS is given by (provided $G_N^{-2/3} \ll \varepsilon \ll 1$)

$$\langle \rho \rangle = 0.97\delta^{-1} G_N^{-1/2} \varepsilon^{-1/4} \exp[-1.93 G_N \varepsilon^{3/2}], \qquad (1)$$

where $\varepsilon = (E_g - E)/E_g$, $G_N = 4\pi\nu D L_y L_z / L_x \gg 1$ is the dimensionless conductance (in units of $e^2/2\pi\hbar$) of the normal part connecting two superconductors, $E_g = 3.12 E_{Th}$, $E_{Th} = D/L_x^2$ is the Thouless energy, and $\delta = (\nu V)^{-1}$ is mean level spacing. Here, L_x is the thickness of the N region, which is assumed to be larger than the superconducting coherence length. It is also assumed that the lateral dimensions L_y, L_z are not much larger than L_x (otherwise, the instanton solution acquires additional dimension(s), and the exponent 3/2 changes; cf. [2] for detail). The corresponding mean-field (MF) expression above the gap is [6]

$$\langle \rho \rangle_{MF} = 3.72\delta^{-1}\sqrt{|\varepsilon|}. \qquad (2)$$

Generally, the functional form of Eqs. (1), (2) is retained, whereas the coefficients are geometry-dependent and can be found from the solution of the standard Usadel equation [11] for a specific sample geometry. In any case, the total number of states with energies below E_g is on the order of unity.

In this letter, we extend our previous results [2] in two different directions. First, we derive *exact* expression for the DOS in the energy region $|\varepsilon| \ll 1$ without

[1] This article was submitted by the authors in English.

the further use of the inequality $\varepsilon \gg G_N^{-2/3}$. The obtained result interpolates smoothly between the semiclassical square-root edge (2) and the exponential tail (1). Second, we consider the same SNS system allowing for nonideal transparencies at the SN interfaces. The result depends upon the relation between the dimensionless interface conductance G_T and normal conductance G_N. As long as $G_T \geq G_N^{1/4}$, all qualitative features of the previous solution are retained but the value of the semiclassical threshold E_g and numerical coefficients in expressions like Eq. (1) become dependent upon the value of $t \equiv G_T/G_N$. However, on further decrease of interface transparency, $G_T \ll G_N^{1/4}$, the DOS behavior changes dramatically: in the semiclassical region $E > E_g$ it acquires the inverse-square-root singularity, $\langle\rho\rangle_{MF} \sim (-\varepsilon)^{-1/2}$. At smallest $|\varepsilon|$, this singularity smoothens out and crosses over to an exponentially decaying tail of low-energy states. A distinctive feature of this tail, as opposed to the situations discussed previously, is that the total number of subgap states becomes large and grows as $G_T^{-1/2} G_N^{1/8} \gg 1$. We coined this situation as "strong tail" and found exponential asymptotic behavior of the DOS in the strong-tail region.

2. Outline of the method. We treat the problem within the supersymmetric formalism. The derivation of the σ-model functional-integral representation can be found in [14, 15, 17]. The DOS is given by the integral over the supermatrix Q:

$$\langle \rho(E, \mathbf{r})\rangle = \frac{\nu}{4}\mathrm{Re}\int \mathrm{str}(k\Lambda Q(\mathbf{r}))e^{-\mathcal{S}[Q]}\mathcal{D}Q, \qquad (3)$$

$$\mathcal{S}[Q] = \frac{\pi\nu}{8}\int d\mathbf{r}\,\mathrm{str}[D(\nabla Q)^2 + 4iQ(\Lambda E + i\tau_x\Delta)]. \qquad (4)$$

Q is an 8×8 matrix operating in Nambu, time-reversal (TR), and Fermi–Bose (FB) spaces. The Pauli matrices operating in the Nambu and TR spaces are denoted by τ_i and σ_i. The matrix k is the third Pauli matrix in the FB space; $\Lambda = \tau_z\sigma_z$. Integration in Eq. (3) runs over the manifold $Q^2 = 1$ with the additional constraint

$$Q = CQ^TC^T, \quad C = -\tau_x\begin{pmatrix} i\sigma_y & 0 \\ 0 & \sigma_x \end{pmatrix}_{FB}. \qquad (5)$$

This manifold is parameterized by eight commuting and eight anticommuting variables. It turns out, however, that only four commuting and four anticommuting modes are relevant in the vicinity of the quasiclassical gap, while contributions from all other modes to the DOS cancel. The detailed discussion of this fact will be published elsewhere [17]. The reduced parameterization for the commuting part of Q in terms of the four variables reads [2]

$$\begin{aligned} Q_c^{BB} &= [\sigma_z\cos k_B + \tau_z\sin k_B(\sigma_x\cos\chi_B + \sigma_y\sin\chi_B)] \\ &\quad\times[\tau_z\cos\theta_B + \sigma_z\tau_x\sin\theta_B], \qquad (6) \\ Q_c^{FF} &= \tau_z\sigma_z\cos\theta_F + \tau_x\sin\theta_F. \end{aligned}$$

The commuting part of the action (with all Grassmann variables being zero) is simplified by introducing new variables $\alpha = (\theta_B + k_B)/2$, $\beta = (\theta_B - k_B)/2$. Then, the action (4) for the normal part ($\Delta = 0$) takes the form

$$S[\theta_F, \alpha, \beta] = 2S_0[\theta_F] - S_0[\alpha] - S_0[\beta], \qquad (7)$$

$$S_0[\theta] = \frac{\pi\nu}{4}\int d\mathbf{r}[D(\nabla\theta)^2 + 4iE\cos\theta]. \qquad (8)$$

Variation of this action yields identical Usadel equations for θ_F, α, and β:

$$D\nabla^2\theta + 2iE\sin\theta = 0, \qquad (9)$$

with the condition $\theta = \pi/2$ at the NS boundaries. Equation (9) generally possesses two different solutions $\theta_{1,2} = \pi/2 + i\psi_{1,2}$, which coincide ($\psi_{1,2}(\mathbf{r}) = \psi_0(\mathbf{r})$) exactly eight at the threshold energy E_g, and are close to each other in the range we are interested in ($|\varepsilon| \ll 1$). Thus, there are possible saddle points for the action (7) corresponding to two solutions of the Usadel equation for each variable θ_F, α, β. Rotation over the angle $\chi_B \in [0, 2\pi)$ connects some of them and produces the whole degenerate family of saddle points (see [2, 17] for detail). In the following, we will need the function $f_0(\mathbf{r})$, which is the normalized difference $\psi_2(\mathbf{r}) - \psi_1(\mathbf{r})$ at $E \longrightarrow E_g$; it obeys the linear equation

$$D\nabla^2 f_0 + 2E_g\sinh\psi_0 f_0 = 0. \qquad (10)$$

3. Exact result for the transparent interface. For energies close to E_g, we substitute $\theta = \pi/2 + i\psi_0 + igf_0$ into Eq. (8), expand it in powers of g and ε, and integrate it over space using Eq. (10):

$$\begin{aligned} S_0[\theta] &= S_0[\pi/2 + i\psi_0] + \tilde{G}\left[-\tilde{\varepsilon}g + \frac{g^3}{3}\right], \\ \tilde{G} &= \frac{\pi c_2 E_g}{2\delta}, \quad \tilde{\varepsilon} = \frac{2c_1}{c_2}\varepsilon. \end{aligned} \qquad (11)$$

Here, we have introduced the constants $c_n = \int (d\mathbf{r}/V) f_0^{2n-1}\cosh\psi_0$. For the quasi-1D geometry, $c_1 = 1.15$ and $c_2 = 0.88$. To describe the deviation of the angles α, β, and θ_F from $\pi/2 + i\psi_0$, we introduce, analogously to g, the three parameters u, v, w, respectively. Grassmann variables are introduced as $Q =$

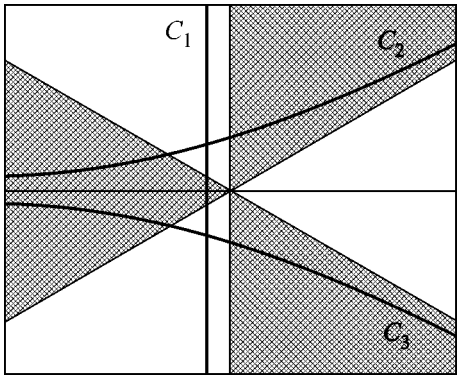

Fig. 1. Possible contours for integration over w and l. The proper choice is C_1 for w and C_3 for l.

$e^{-iW_c/2}e^{-iW_a/2}\Lambda e^{iW_a/2}e^{iW_c/2}$, where $Q_c = e^{-iW_c/2}\Lambda e^{iW_c/2}$ is specified in Eqs. (6) and

$$W_a = \begin{pmatrix} 0 & W_a^{\mathrm{FB}} \\ i\tau_x\sigma_x(W_a^{\mathrm{FB}})^T\sigma_y\tau_x & 0 \end{pmatrix},$$

as it must satisfy the anti-self-conjugate condition $W_a + CW_a^T C^T = 0$. Finally,

$$W_a^{\mathrm{FB}} = \frac{f_0}{4}\begin{pmatrix} 0 & \zeta-\lambda & \zeta+\lambda & 0 \\ -\zeta+\lambda & 0 & 0 & -\zeta-\lambda \\ \xi+\eta & 0 & 0 & \xi-\eta \\ 0 & -\xi-\eta & -\xi+\eta & 0 \end{pmatrix}.$$

Expansion of the action in u, v, w and Grassmann variables leads to

$$\mathcal{S} = \tilde{G}\Big[\tilde{\varepsilon}(u+v-2w) - \frac{u^3-v^3-2w^3}{3} - \zeta\xi\frac{u+w}{4} - \lambda\eta\frac{v+w}{4}\Big]. \quad (12)$$

For calculating the DOS, we also need an expansion of the preexponential factor in Eq. (3) as well as the Jacobian J for the parameterization of the Q matrix:

$$\frac{\nu}{4}\int d\mathbf{r}\,\mathrm{str}(k\Lambda Q) = -\frac{ic_1}{2\delta}(u+v+2w),$$

$$J = \frac{8i\tilde{G}^2}{\pi}|u-v|.$$

By integrating over Grassmann variables and the cyclic angle χ_B, performing a rescaling $(u, v, w) \longrightarrow (2\tilde{G})^{-1/3}(u, v, w)$, which excludes $\tilde{G}$ from the integrand, and changing the variables to $l = (u+v)/2$, $m = (u-v)^2/2$, we arrive at the following expression for the integral DOS:

$$\langle\rho\rangle = \frac{c_1(2\tilde{G})^{-1/3}}{4\pi\delta}\mathrm{Re}\int_0^\infty dm\int dl\,dw(w+l) \times (w^2+2lw+l^2-m)\exp\Big[-\frac{w^3}{3}+\epsilon w+\frac{l^3}{3}+ml-\epsilon l\Big], \quad (13)$$

where we introduced the notation $\epsilon = (2\tilde{G})^{2/3}\tilde{\varepsilon}$.

At this stage, we have to choose the contours of integration over w and l. The usual convergence requirements for the nonexpanded action (7) force the contour for w (l) to go along the imaginary (real) axis at large values of w (l). However, since the main contribution to the DOS comes from Eq. (13) determined by small w and l, these contours should be properly deformed to achieve convergence of Eq. (13). The integral (13) converges if the contour for l runs to infinity in the dark regions in Fig. 1, and otherwise for w. Therefore, we should choose the contour C_1 for w (see Fig. 1), whereas for l there are two possibilities: C_2 and C_3. The correct choice is dictated by the positivity of the DOS, which implies the contour C_3 for l. Integration in Eq. (13) is straightforward although rather cumbersome and leads to the final expression for the DOS:

$$\langle\rho\rangle = \frac{2\pi c_1}{(2\tilde{G})^{1/3}\delta} \times\Big[-\epsilon\mathrm{Ai}^2(\epsilon)+[\mathrm{Ai}'(\epsilon)]^2+\frac{\mathrm{Ai}(\epsilon)}{2}\int_{-\infty}^{\epsilon}dy\,\mathrm{Ai}(y)\Big], \quad (14)$$

where $\mathrm{Ai}(\epsilon)$ is the Airy function. Asymptotic behavior of the calculated DOS at $\epsilon \gg 1$ coincides with the result (1) of the single-instanton approximation [2]; see Fig. 2.

The functional dependence (14) coincides with the RMT prediction for the spectrum edge in the orthogonal ensemble [12]. It is not surprising, because the random-matrix theory is known to be equivalent to the 0D σ model [14]. In our case, the problem became effectively 0D after we had fixed the coordinate dependence $f_0(\mathbf{r})$ for the parameters of Q near E_g.

Breaking the time-reversal symmetry drives the system to the unitary universality class. The corresponding RMT result [12] can be obtained from Eq. (14) by dropping the last integral term. This result can easily be derived by the σ-model analysis in the following way. A strong magnetic field imposes an additional constraint on the Q matrix. As a result, the mode associated with the variable m acquires a mass; so, instead of integrating over it we set $m = 0$. One of the Grassman modes is also frozen out, giving the preexponent (w +

$l)^2$ in the integral (13). Finally, the expression for DOS coincides with Eq. (14) without the last term.

4. Finite transparency of the NS interface. We now turn to the analysis of the subgap structure of a quasi-1D SNS contact with finite conductance G_T of the NS boundary. The role of the interface is described by the dimensionless parameter $t = G_T/G_N$. For $t \gg 1$, the interface is transparent and the result (14) applies. In what follows, we will consider the case $t \ll 1$. The effect of finite transparency is described by the additional boundary term [14] in the action

$$\mathcal{S}_{\text{boundary}} = -\frac{G_T}{16}\text{str}(Q^L Q^R), \tag{15}$$

where $Q^{L,R}$ are the Q matrices at both sides of the interface. Equation (15) is the first term in the expansion of the general boundary action [4, 14, 18] in the small transparency $\Gamma \ll 1$ of the conductive channel and leads to the Kupriyanov–Lukichev [19] boundary conditions. In the diffusive regime ($l \ll L_x$) at $t \ll 1$, we have $\Gamma \sim tl/L_x$, which justifies the use of Eq. (15). The commuting part of the action can still be written in the form (7) with the additional term in S_0:

$$S_0[\theta] = \frac{\pi\nu L_y L_z}{4}\int_{-L_x/2}^{L_x/2} dx[D(\theta')^2 + 4iE\cos\theta] - \frac{G_T}{4}\sin\left[\theta\left(\frac{L_x}{2}\right)\right]. \tag{16}$$

In the limit $t \ll 1$, the Usadel equation has almost spatially homogeneous solutions, which allows the use of the expansion $\psi = A + B[1 - 4(x/L_x)^2]$ for them. Substituting this ansatz into the action (16) and minimizing over B, we obtain the action in terms of $P = e^A$:

$$S_0(P) = \frac{G_N}{8}\left[(s-t)P - \frac{2t}{P} + \frac{t^2}{24}P^2\right], \tag{17}$$

where $s = E/E_{Th}$. Here, we keep only leading terms and substitute t for all s, except for the first one. After variation, we find the cubic saddle-point equation for P:

$$\frac{s}{t} = 1 - \frac{2}{P^2} - \frac{t}{12}P. \tag{18}$$

The maximum of the RHS, achieved at $P_0 = (48/t)^{1/3}$, determines the position of the mean-field gap: $s_g = t + O(t^{5/3})$ and, hence, $E_g = G_T\delta/4\pi$. Depending on the deviation from the threshold, $\varepsilon = (E_g - E)/E_g = (s_g - s)/s_g$, there are two regimes for Eq. (18).

Weak tail. If $|\varepsilon| \ll t^{2/3}$, the two solutions to Eq. (18) are close to each other and can be sought in the form $P = P_0 + \delta P$. Expanding the action in powers of δP, we get

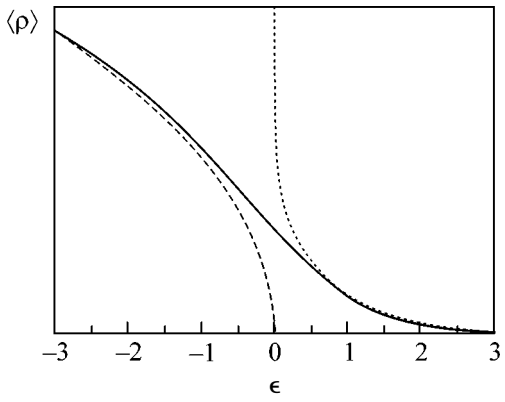

Fig. 2. (Solid line) Exact dependence (14) of the DOS on the dimensionless energy ϵ, (dotted line) single-instantion approximation (1), and (dashed line) semiclassical result (2) for the DOS.

$$S_0(P) = S_0(P_0) + \frac{G_T}{8}\left[-\varepsilon\delta P + \frac{2}{P_0^4}(\delta P)^3\right]. \tag{19}$$

This equation closely resembles its counterpart (11) for the transparent interface. As mentioned in [4], this form of the expansion of the action in powers of small deviations near the threshold solution inevitably leads to the instanton action scaling as $\varepsilon^{3/2}$. In fact, there is full equivalence [17] between the DOS for the transparent NS interface given by Eq. (14) and the DOS in the limit $|\varepsilon| \ll t^{2/3} \ll 1$. The latter can be obtained from the former by redefinition of the constants $c_{1,2}$. For a 1D planar contact, they appear to be $c_1 = P_0/2$, $c_2 = 6/P_0$, $E_g/E_{Th} = t$.

In particular, above the threshold, at $\varepsilon < 0$, one encounters the mean-field square-root singularity

$$\langle\rho\rangle_{MF} = \frac{4}{\delta}\frac{6^{1/6}}{t^{2/3}}\sqrt{|\varepsilon|}. \tag{20}$$

The instanton action becomes $\mathcal{S} = S_0(P_1) - S_0(P_2) = (2/3)6^{1/6}G_N t^{1/3}\varepsilon^{3/2}$, and the single-instanton asymptotic form of the DOS tail reads

$$\langle\rho\rangle = \frac{1}{\delta}\sqrt{\frac{\pi 6^{1/6}}{2G_N t^{5/3}\sqrt{\varepsilon}}}\exp\left(-\frac{2}{3}6^{1/6}G_N t^{1/3}\varepsilon^{3/2}\right). \tag{21}$$

Strong tail. In the opposite limit, $t^{2/3} \ll |\varepsilon| \ll 1$, the difference between the two solutions to Eq. (18) is large but expansion (17) is still valid (gradients of $\psi_{1,2}$ are small, provided $\varepsilon \ll 1$). The roots $P_{1,2}$ can be found by neglecting either the second or the third term in Eq. (18): $P_1 = \sqrt{2/\varepsilon}$, $P_2 = 12\varepsilon/t$, with $P_2 \gg P_1$. Above

References to the asymptotic formulas for the DOS above ($\varepsilon < 0$) and below ($\varepsilon > 0$) the gap, and the width $|\varepsilon|_{\text{fluct}}$ of the fluctuation region for the regimes of the transparent interface ($t \gg 1$), weak ($|\varepsilon| \ll t^{2/3} \ll 1$) and strong ($t^{2/3} \ll |\varepsilon| \ll 1$) tails

	$\varepsilon < 0$	$\varepsilon > 0$	$\lvert\varepsilon\rvert_{\text{fluct}}$
$t \gg 1$	(2)	(1)	$G_{\text{N}}^{-2/3}$
$\lvert\varepsilon\rvert \ll t^{2/3} \ll 1$	(20)	(21)	$G_{\text{N}}^{-2/3}\, t^{-2/9}$
$t^{2/3} \ll \lvert\varepsilon\rvert \ll 1$	(22)	(23)	$G_{\text{N}}^{-1/2}$

the threshold, this gives the inverse-square-root singularity in the semiclassical DOS:

$$\langle\rho\rangle_{\text{MF}} = 2\nu\text{Re}\int d\mathbf{r}\cos\theta = \frac{1}{\delta}\text{Im}(P - P^{-1}) = \frac{1}{\delta}\sqrt{\frac{2}{|\varepsilon|}}. \quad (22)$$

Below E_g, one obtains for the instanton action $\mathcal{S} = -S_0(P_2) = (3/4)G_{\text{N}}\varepsilon^2$, which determines the one-instanton asymptotics of the subgap DOS. The preexponent can be calculated by generalizing the method of [2]. Introducing the deviation parameter q according to $\alpha = \pi/2 + i\log P_2 + iq/\sqrt{2}$ and expanding the action in powers of q and the corresponding Grassmann pair $\zeta\xi$, we obtain for the action and the preexponential factor in Eq. (3)

$$\mathcal{S} = \frac{3}{8}G_{\text{N}}\varepsilon^2\left[2 - q^2 + \frac{q\zeta\xi}{2\sqrt{2}}\right],$$

$$\frac{\nu}{4}\int d\mathbf{r}\,\text{str}(k\Lambda Q) = -\frac{3i\varepsilon}{t\delta}\left[1 - \frac{q}{\sqrt{2}}\right].$$

The measure of integration is $\mathcal{D}Q = 2\sqrt{3/t}\,(2\varepsilon)^{3/4}dqd\zeta d\xi$. Inserting these into Eq. (3), we finally obtain

$$\langle\rho\rangle = \frac{3}{\delta}\sqrt{\frac{\pi}{G_{\text{N}}t^3}}\sqrt{\frac{\varepsilon^3}{2}}\exp\left(-\frac{3}{4}G_{\text{N}}\varepsilon^2\right). \quad (23)$$

5. Discussion. We have considered the integral density of states in a coherent diffusive SNS junction with an arbitrary transparency of the SN interface. For the ideal interface ($G_{\text{T}} \gg G_{\text{N}}$), we managed to go beyond the single-instanton analysis [2] and derived the exact result (14), which is valid as long as $|E - E_g| \ll E_g$. This expression uniquely describes the semiclassical square-root DOS (2) above the Thouless gap E_g, the far subgap tail (1), and the crossover region $\varepsilon \sim G_{\text{N}}^{-2/3}$ between the two asymptotic expressions. The functional form of this result coincides with the prediction of the RMT.

As the SN interface becomes less transparent, $G_{\text{T}} \ll G_{\text{N}}$, the situation changes. At $G_{\text{T}} \gg G_{\text{N}}^{1/4}$, these changes are only quantitative: the position of the quasiclassical gap is shifted to $E_g = (G_{\text{T}}/G_{\text{N}})E_{\text{Th}}$, but the DOS both above [Eq. (20)] and below [Eq. (21)] the gap has the same dependence on the deviation ε from E_g, with the coefficients becoming dependent on G_{T}. In this limit, the very far part of the tail [at $\varepsilon \gg (G_{\text{T}}/G_{\text{N}})^{2/3}$] exhibits a different ε dependence (23), but the corresponding DOS is exponentially small. Therefore, in the limit $G_{\text{T}} \gg G_{\text{N}}^{1/4}$, the total number of subgap states is on the order of 1 and independent of G_{T}. We refer to this case as weak tail.

As the interface becomes less transparent, the region of applicability of the weak tail shrinks and finally disappears at $G_{\text{T}} \sim G_{\text{N}}^{1/4}$. For even lower $G_{\text{T}} \ll G_{\text{N}}^{1/4}$, the difference between the case of the transparent interface becomes qualitative: the DOS above E_g acquires an inverse square-root dependence (22), while the subgap DOS follows Eq. (23). In this regime, the total number of subgap states is proportional to $G_{\text{T}}^{-1/2}\, G_{\text{N}}^{1/8} \gg 1$ and grows with decreasing G_{T}, in contrast to all previous cases where this number is on the order of 1. This indicates that at $G_{\text{T}} \sim G_{\text{N}}^{1/4}$ the universality class of the problem changes. At $G_{\text{T}} \ll G_{\text{N}}^{1/4}$, it is no longer equivalent to the spectral edge of the Wigner–Dyson random-matrix ensembles.

The asymptotic results for the DOS above and below the gap, as well as the width of the fluctuation region near E_g, are summarized in the table for the three regions considered.

This work was supported by the SCOPES program of Switzerland, the Dutch Organization for Fundamental Research (NWO), the Russian Foundation for Basic Research (project no. 01-02-17759), the program "Quantum Macrophysics" of the Russian Academy of Sciences, and the Russian Ministry of Science. MAS was supported in part by the Russian Science Support Foundation.

REFERENCES

1. M. G. Vavilov, P. W. Brower, V. Ambegaokar, and C. W. J. Beenakker, Phys. Rev. Lett. **86**, 874 (2001).
2. P. M. Ostrovsky, M. A. Skvortsov, and M. V. Feigel'man, Phys. Rev. Lett. **87**, 027002 (2001).
3. A. Lamacraft and B. D. Simons, Phys. Rev. Lett. **85**, 4783 (2000).
4. A. Lamacraft and B. D. Simons, Phys. Rev. B **64**, 014514 (2001).
5. A. A. Golubov and M. Yu. Kupriyanov, Zh. Éksp. Teor. Fiz. **96**, 1420 (1989) [Sov. Phys. JETP **69**, 805 (1989)].
6. F. Zhou, P. Charlat, B. Spivak, and B. Pannetier, J. Low Temp. Phys. **110**, 841 (1998).
7. J. A. Melsen, P. W. Brower, K. M. Frahm, and C. W. J. Beenakker, Europhys. Lett. **35**, 7 (1996); Phys. Scr. **69**, 223 (1997).

8. S. Pilgram, W. Belzig, and C. Bruder, Phys. Rev. B **62**, 12462 (2000).
9. G. Eilenberger, Z. Phys. **214**, 195 (1968).
10. A. I. Larkin and Yu. N. Ovchinnikov, Zh. Éksp. Teor. Fiz. **55**, 2262 (1968) [Sov. Phys. JETP **28**, 1200 (1969)].
11. K. Usadel, Phys. Rev. Lett. **25**, 507 (1970).
12. C. A. Tracy and H. Widom, Commun. Math. Phys. **159**, 151 (1994); **177**, 727 (1996).
13. M. L. Mehta, *Random Matrices* (Academic, New York, 1991).
14. K. B. Efetov, *Supersymmetry in Disorder and Chaos* (Cambridge Univ. Press, New York, 1997).
15. A. Altland, B. D. Simons, and D. Taras-Semchuk, Pis'ma Zh. Éksp. Teor. Fiz. **67**, 21 (1997) [JETP Lett. **67**, 22 (1997)]; Adv. Phys. **49**, 321 (2000).
16. B. A. Muzykantskii and D. E. Khmelnitskii, Phys. Rev. B **51**, 5480 (1995).
17. P. M. Ostrovsky, M. A. Skvortsov, and M. V. Feigel'man, Zh. Éksp. Teor. Fiz. (in press) [JETP (in press)].
18. W. Belzig and Yu. V. Nazarov, Phys. Rev. Lett. **87**, 067006 (2001).
19. M. Yu. Kuprianov and V. F. Lukichev, Zh. Éksp. Teor. Fiz. **94** (6), 139 (1988) [Sov. Phys. JETP **67**, 1163 (1988)].